Lipid Binding of the Exchangeable Apolipoprotein Apolipophorin III Induces Major Changes in Fluorescence Properties of Tryptophans 115 and 130†

Paul M. M. Weers,‡ Elmar J. Prenner,§ Cyril Kay,§ and Robert O. Ryan*,‡

Lipid Biology Research Group and Protein Engineering Network of Centres of Excellence, Department of Biochemistry, University of Alberta, Edmonton, Alberta, T6G 2S2 Canada

Received December 16, 1999; Revised Manuscript Received March 17, 2000

ABSTRACT: The effect of lipid association on the local environment of the two tryptophan residues of *Locusta migratoria* apolipophorin III (apoLp-III) has been studied. In the lipid-free state, Trp115 in helix 4 is buried in the hydrophobic interior of the helix bundle, while Trp130 is located in a loop connecting helices 4 and 5. Fluorescence spectroscopy of single Trp mutants revealed an emission maximum (λ_{max}) of 321 nm for apoLp-III−W@115 (excitation 280 nm) which red-shifted to 327 nm upon binding to dimyristoylphosphatidylcholine (DMPC). ApoLp-III−W@130 displayed a λ_{max} of 338 nm while interaction with DMPC resulted in a blue shift to 331 nm. Quenching studies with KI and acrylamide revealed decreased accessibility to Trp115 compared to Trp130, while lipid binding induced a decrease in quenching of Trp130. Aromatic circular dichroism (CD) spectra showed that Trp vibronic transitions at 278, 286, and 294 nm for lipid-free apoLp-III were caused by Trp115. Upon lipid association, aromatic extrema are reversed in sign, becoming entirely negative with both Trp residues contributing to the vibronic transitions, implying restriction in side-chain mobility of these residues. Thus, λ_{max}, quencher accessibility, and aromatic CD analysis indicate that Trp115 is much less solvent-exposed than Trp130. Differences in fluorescence properties of these residues are minimized in the lipid-bound state, a result of relocation of Trp115 and Trp130 into the lipid milieu. Thus, in addition to the hydrophobic faces of apoLp-III amphipathic α-helices, the loop region containing Trp130 comes in close contact with DMPC.

Apolipophorin III (apoLp-III)[1] from *Locusta migratoria* is an exchangeable apolipoprotein that binds reversibly to lipoprotein surfaces and is used as a model for studying structure−function relationships of exchangeable apolipoproteins (*1*−*3*). It is one of the few apolipoproteins for which high-resolution structural data have been reported (*4*). Other examples are the N-terminal domain of human apolipoprotein (apo) E (*5*), human (Δ1−43)apoA-I (*6*), and apoLp-III from *Manduca sexta* (*7*). Since each of these structures was obtained in the absence of lipid, there remains a gap in our understanding of the lipid-bound conformation of exchangeable apolipoproteins. It is thought that reorganization of helical segments allows direct interaction of the hydrophobic face of apolipoprotein amphipathic α-helices with the lipid milieu (*4, 8*−*11*). The 3D structure of *L. migratoria* apoLp-III together with a highly efficient recombinant expression system (*12, 13*) have facilitated study of how this protein interacts with lipids, providing useful insight into exchangeable apolipoprotein function (*14*−*17*). In the lipid-free state apoLp-III is composed of five amphipathic α-helices organized as an up-and-down helix bundle, exposing hydrophilic amino acid side chains while burying most of its hydrophobic residues. Upon recognition of hydrophobic surface defects on lipoproteins, the protein associates with the lipoprotein surface by adopting an open conformation that exposes a hydrophobic continuum that contacts the surface of the lipoprotein particle (*4, 11, 16*−*19*). Of its 164 amino acids *L. migratoria* apoLp-III contains four aromatic residues, two Trp and two Phe. The Trp residues provide intrinsic probes to monitor changes in protein conformation during interaction with lipids. Interpretation of apoLp-III Trp fluorescence spectra are simplified by the lack of Tyr, allowing excitation at the Trp excitation maximum of 280 nm. The lack of Tyr and Cys also contributes to the well-defined aromatic circular dichroism (CD) spectrum observed for this apolipoprotein (*19*). Trp115 is localized in the middle of helix 4 (Figure 1), while the loop connecting helices 4 and 5 bears Trp130, providing probes localized to an α-helical segment and a loop segment. To investigate the effect of lipid binding on these Trp residues, Trp115 or Trp130 was replaced by Phe to create single-Trp apoLp-IIIs. Major differences were observed in the fluorescence properties of apoLp-III−W@115 and apoLp-III−W@130 in the lipid-free state, reflecting their different locations in the globular helix bundle. However, lipid association caused both fluorophores to reorient to a similar lipid environment. The fluorescence properties of this model exchangeable apolipoprotein provide insights into the molecular adaptation of apoLp-III upon the transition from a lipid-free to a lipid-bound state.

† Supported by a grant from the Medical Research Council of Canada.

* To whom correspondence should be addressed at the Lipid and Biology Research Group, University of Alberta, 328 Heritage Medical Research Centre, Edmonton, Alberta, T6G 2S2 Canada. Tel (780) 492-5153; fax (780) 492-3383; e-mail robert.ryan@ualberta.ca.

‡ Lipid Biology Research Group.

§ Protein Engineering Network of Centres of Excellence (PENCE).

[1] Abbreviations: apoLp-III, apolipophorin III; apo, apolipoprotein; DMPC, dimyristoylphosphatidylcholine; CD, circular dichroism; λ_{max}, emission maximum.

10.1021/bi992891x CCC: $19.00
Published on Web 05/18/2000

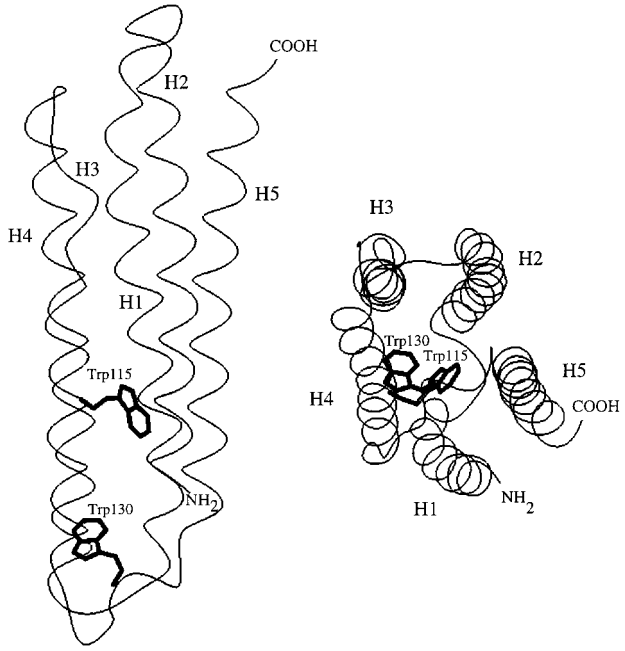

FIGURE 1: Ribbon diagram of the structure of *L. migratoria* apoLp-III according to Breiter et al. (*4*). The position of Trp115 in helix 4 (H4) and Trp130 in the loop connecting helices 4 and 5 are indicated in the side view (left) and end-on view looking from the COOH-terminal end of the protein (right).

MATERIALS AND METHODS

Site-Directed Mutagenesis and Overexpression of Recombinant Proteins. Site-directed mutagenesis was performed with the pALTER system (Promega, Madison, WI). Primers designed to substitute Trp115 or Trp130 with Phe were annealed with single-stranded template DNA followed by ligation by T4 ligase. The DNA mixture was used to transform *mutS Escherichia coli* cells, and grown overnight in LB medium containing 125 μg/mL ampicillin. Plasmid DNA was extracted and used to transform JM109 cells. Selected colonies were grown in LB with 50 μg/mL ampicillin, and plasmid DNA was extracted and sequenced by the dideoxynucleotide chain-termination method (*20*) to confirm the presence of the desired mutation. *E. coli* BL21-(DE3) cells were used for overexpression of the wild-type and mutant proteins (*13*). Overnight cultures in LB were used to seed M9 minimal medium (1 L) at 37 °C until an OD_{600} of 0.6 was reached, and apoLp-III expression induced with isopropyl β-D-thiogalactopyranoside (1 mM final concentration). After 4 h, cells were pelleted and recombinant apoLp-III was isolated from the cell-free supernatant by preparative reversed-phase HPLC (Beckman) on a Zorbax column (RXC-8). Proteins were eluted with a linear gradient of water−acetonitrile (0.05% TFA). The purity of the samples was analyzed by analytical reversed-phase HPLC. Proteins were subjected to electrospray ionization mass spectrometry to confirm the presence of the mutation (VG Quattro electrospray mass spectrometer, Fisons Instruments, Manchester, U.K.). A decrease of 38 ± 2 Da was observed for both mutant proteins, in agreement with the expected difference in mass between Trp and Phe residues (39 Da).

Trypsin Digestion. Peptide fragments of wild-type apoLp-III, each containing one tryptophan residue, were obtained by trypsin digestion. Five milligrams of apoLp-III was cleaved with 20 μg of porcine sequencing-grade modified trypsin (Promega) for 16 h at 37 °C in 50 mM NH_4HCO_3. Fragments were separated by reversed-phase HPLC and identified by electrospray ionization mass spectrometry. The mass of the peptide comprising residues 83−121 (including Trp115) was 4275 ± 6 Da (expected mass 4274.6 Da) and for peptide 122−143 (bearing Trp130) a mass of 2314 ± 1 Da was obtained (expected mass 2314.5 Da).

Phospholipid Vesicle Clearance. Five milligrams of dimyristoylphosphatidylcholine (DMPC, Avanti Polar Lipids Inc., Alabaster, AL) were dissolved in a mixture of chloroform and methanol (3:1 v/v) and dried under a stream of N_2. One milliliter of prewarmed buffer was added (20 mM Tris-HCl, pH 7.2, 150 mM NaCl, and 0.5 mM EDTA) and vortexed for 1 min. Unilamellar vesicles were prepared by extrusion through a 200 nm membrane (Avanti Polar Lipids Inc). Light scattering was used to monitor apoLp-III-induced transformation of vesicles into discoidal complexes (*21*). To a thermostated 1-mL cuvette, buffer, 250 μg of vesicles and 250 μg of apoLp-III (resulting in a lipid:protein molar ratio of 26:1) was added and clearance of the solution was monitored by light scattering in a Perkin-Elmer spectrofluorometer (model LS 50B). Excitation and emission wavelengths were set at 600 nm with a slit width of 3 nm. The temperature of the cuvette was maintained at 24 °C. All solutions were preincubated at this temperature. First-order rate constants (k) were obtained from the slope of a plot of the logarithm of light scatter intensity versus time.

Circular Dichroism. Circular dichroism (CD) measurements were carried out on a Jasco J-720 spectropolarimeter (Jasco Inc., Easton, MD) interfaced to an Epson Equity 386/25 computer controlled by Jasco software to analyze secondary structure content, to monitor guanidine hydrochloride-induced denaturation, and to obtain near-UV spectra as described previously (*19*).

Fluorescence Studies. Fluorescence experiments were carried out on a Perkin-Elmer LS 50B spectrofluorometer. Temperature was controlled at 20 °C in a thermostated cell holder. Excitation was set at 280 nm with a slit width of 3.5 nm, and emission was monitored between 290 and 450 nm. The quantum yield of apoLp-III samples in the absence or presence of DMPC was calculated from the following equation: $Q_u = (Q_s A_u OD_s)/(A_s OD_u)$, where Q_u = quantum yield of unknown apoLp-III samples, $Q_s = 0.13$ represents the quantum yield of (standard) free L-Trp (*22*), A_s and A_u represent total fluorescence emission of L-Trp or apoLp-III samples, and OD_s and OD_u represent absorbance of L-Trp or apoLp-III samples at 280 nm (corrected for light scattering). All fluorescence measurements were carried out in 50 mM sodium phosphate buffer, pH 7.5.

For quenching studies with KI and acrylamide, protein samples were excited at 295 nm to minimize absorbance of the quencher, and emission was monitored at their λ_{max} (*23*). An absorbance correction was used for acrylamide of log $A/2$ at 295 nm, and all readings were corrected for dilution. The solution of KI contained 1 mM sodium thiosulfate to prevent formation of free iodine. The data were analyzed by use of the Stern−Volmer equation: $F_0/F = 1 + K_{sv}[Q]$, where F_0 and F represent the emission maximum in the absence and presence of quencher, respectively. The collisional quenching constant (K_{sv}) was determined from the initial slope of plots of F_0/F versus [Q].

Table 1: Structural and Functional Properties of Wild-Type and Mutant ApoLp-IIIs

apoLp-III	$[GdnHCl]_{1/2}$[a] (M)	$\Delta G_D^{H_2O}$[b] (kcal/mol)	k[c] (s^{-1})
wild type[d]	0.58	2.7	6.1×10^{-4}
W@115	0.42	2.0	5.4×10^{-4}
W@130	0.52	2.1	5.0×10^{-4}

[a] $[GdnHCl]_{1/2}$ is the transition midpoint, the molar concentration of guanidine hydrochloride required to achieve 50% of the maximal decrease in ellipticity at 221 nm. [b] $\Delta G_D^{H_2O}$ is the free energy of unfolding in the absence of guanidine hydrochloride. [c] Rate constants (k) of the transformation of DMPC vesicles into discoidal apoLp-III−DMPC complexes were obtained from the slope of the logarithm of light scatter intensity versus time. [d] Data from Weers et al. (*13*).

RESULTS

Characterization of Mutant ApoLp-IIIs. To create single-Trp apoLp-IIIs, two mutants were designed wherein Trp115 or Trp130 was changed to a Phe. For the W115F mutation, the mutant protein bears a single Trp in position 130 and thus is termed apoLp-III−W@130. Likewise, the W130F mutant is termed apoLp-III−W@115. Mutant and wild-type proteins were overexpressed in *E. coli* and purified by reversed-phase HPLC (*13*). The structural and stability properties of these proteins were studied by CD spectroscopy and GdnHCl-induced denaturation. Far-UV CD spectral analysis showed a high α-helical content for both mutant apoLp-IIIs similar to that of wild-type apoLp-III (*19*). Midpoints of GdnHCl denaturation of apoLp-III−W@115 and apoLp-III−W@130 were 0.42 and 0.52 M, comparable with those of wild-type apoLp-III (Table 1). $\Delta G_D^{H_2O}$ values of the mutants were in the same range as that of wild-type apoLp-III, indicating the conservative mutations introduced did not affect the stability properties of the protein.

To assess protein function, the ability of apoLp-III to transform DMPC vesicles to discs was evaluated. The DMPC vesicle preparation (approximately 200 nm in diameter) has a turbid appearance, which, at 24 °C, clears rapidly upon addition of apoLp-III due to transformation into much smaller discoidal DMPC−apoLp-III complexes (14 nm average diameter; *19*). This spontaneous clearance can be conveniently monitored by right-angle light scattering spectroscopy. As seen in Figure 2, wild-type apoLp-III interacts strongly with the vesicles as demonstrated by the rapid decrease in light scattering, yielding a first-order rate constant (k) of 6.1×10^{-4} s^{-1}. In the absence of apoLp-III the dispersion of DMPC vesicles remains turbid. Addition of apoLp-III−W@115 or apoLp-III−W@130 to the vesicle dispersion resulted in sample clearance at rates that were similar to that for wild-type protein, indicating the mutant proteins are functional (Table 1). Far-UV CD spectra of the proteins complexed to DMPC showed high α-helical content with no differences between wild-type and the single-Trp mutants (not shown).

Emission Spectra. Excitation of lipid-free wild-type apoLp-III at 280 nm yielded an emission λ_{max} of 332 nm, the result of the sum of the fluorescence emission of the two tryptophan residues. ApoLp-III−W@115 has a λ_{max} of 321 nm, indicating it is localized in a nonpolar environment. On the other hand, apoLp-III−W@130 resides in a more polar environment as indicated by a λ_{max} of 338 nm (Figure 3A). In addition to use of free L-Trp as a reference, Trp residues present in an unstructured protein environment were evaluated. Two peptides of 39 and 22 residues, each containing one of the Trp residues in intact wild-type apoLp-III, were generated by trypsin digestion. Peptide I encompasses residues 83−121 and includes Trp115, while peptide II encompasses residues 122−143 and bears Trp130. Both showed a λ_{max} of ∼350 nm, similar to that of free L-Trp, implying full exposure of the fluorophores to the aqueous buffer (Table 2). Association of wild-type apoLp-III with DMPC resulted in a slightly lower emission maximum (shifted from 332 to 329 nm). However, this small blue shift was the result of opposing emission shifts of the tryptophan residues, as seen by examination of the single-tryptophan mutants. Whereas apoLp-III−W@130 undergoes a 7 nm blue shift upon lipid interaction, apoLp-III−W@115 undergoes a 6 nm red shift (Figure 3B). The initial 17 nm difference between the two mutants was reduced to 4 nm upon lipid binding, indicating the Trp residues relocate to similar environments.

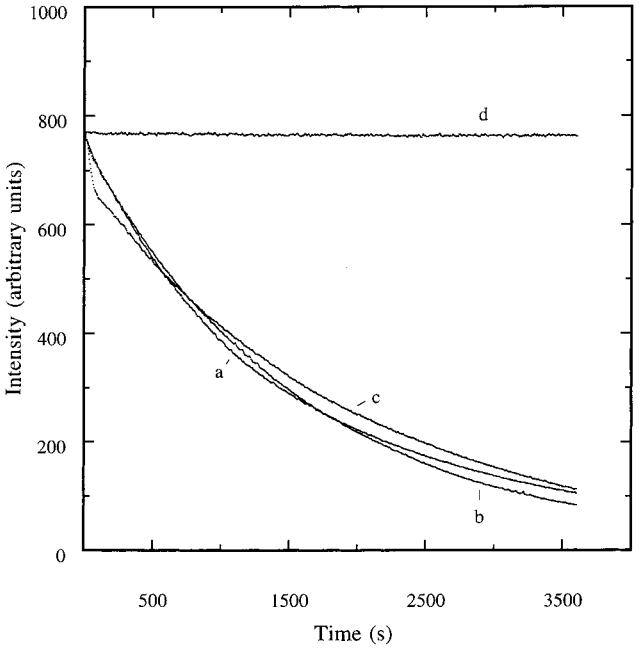

FIGURE 2: Clearance of DMPC vesicles by wild-type and mutant apoLp-IIIs. Vesicles were transformed into the smaller disclike complexes by addition of wild-type apoLp-III (curve a), apoLp-III−W@115 (curve b), or apoLp-III−W@130 (curve c) at a lipid:protein molar ratio of 26:1. Vesicles in the absence of apoLp-III remained turbid (curve d). Incubations were carried out at 24 °C. Sample turbidity was monitored by right-angle light scattering as a function of time.

Quantum yields of the single tryptophan mutants were higher compared to that of free L-Trp. When Trp was part of a peptide, the lowest quantum yield was obtained (Table 2). Association of wild-type or mutant apoLp-IIIs with DMPC resulted in decreased quantum yields, with the decrease observed for apoLp-III−W@115 being smaller than that for wild-type and apoLp-III−W@130.

Quenching Studies with KI and Acrylamide. Fluorescence quenching experiments were performed to obtain additional information about the local environment of Trp115 and Trp130. Acrylamide was selected as a neutral quencher and KI as a negatively charged quencher. CsCl, employed as a positively charged quencher, was unable to quench Trp fluorescence of apoLp-III (not shown). Stern−Volmer plots

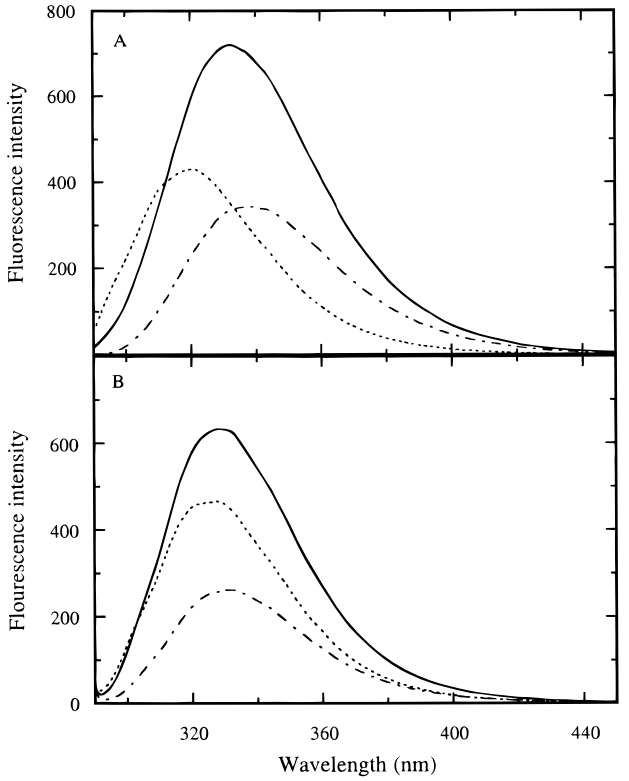

FIGURE 3: Trp fluorescence spectroscopy of apoLp-III. (A) Emission spectra in the lipid-free state. Twenty micrograms of wild-type apoLp-III (—), apoLp-III−W@115 (- - -), or apoLp-III−W@130 (-•-) was excited at 280 nm (slit width 3.5 nm), and fluorescence emission was monitored between 290 and 450 nm. (B) Emission spectra of wild-type and mutant apoLp-IIIs complexed with DMPC.

Table 2: Trp Fluorescence of ApoLp-IIIs

protein	λ_{max}[a]	quantum yield
wild type	332	0.185
wild type−DMPC	329	0.120
W@115	321	0.177
W@115−DMPC	327	0.142
W@130	338	0.167
W@130−DMPC	331	0.096
free L-Trp[b]	351	0.130
peptide I [83−121]	349	0.064
peptide II [122−143]	351	0.059

[a] ±1 nm. [b] Obtained from Provencher and Glöckner (*22*).

were linear for KI (Figure 4) and acrylamide (Figure 5). K_{sv} constants for KI quenching of the single-tryptophan proteins in the lipid-free state were obtained from the initial slope of Stern−Volmer plots; they varied between 0.42 M^{-1} for apoLp-III−W@115 and 2.25 M^{-1} for apoLp-III−W@130. In the case of wild-type apoLp-III, a K_{sv} constant of 1.35 M^{-1} was obtained (Table 3). In the lipid-bound state (Figure 4B), K_{sv} constants were significantly reduced for apoLp-III−W@130 and, consequently, wild-type apoLp-III. All three DMPC-bound proteins displayed similar K_{sv} values and were in the range of 0.5−0.7 M^{-1}. When acrylamide was employed as a quencher, a similar trend was observed (Figure 5A). ApoLp-III−W@115 yielded the lowest K_{sv} constant (0.94 M^{-1}), while apoLp-III−W@130 was the most accessible for quenching (K_{sv} = 3.17 M^{-1}). The wild-type protein showed a K_{sv} constant that equaled the average of the two mutant apoLp-IIIs (1.96 M^{-1}). Association with lipid resulted

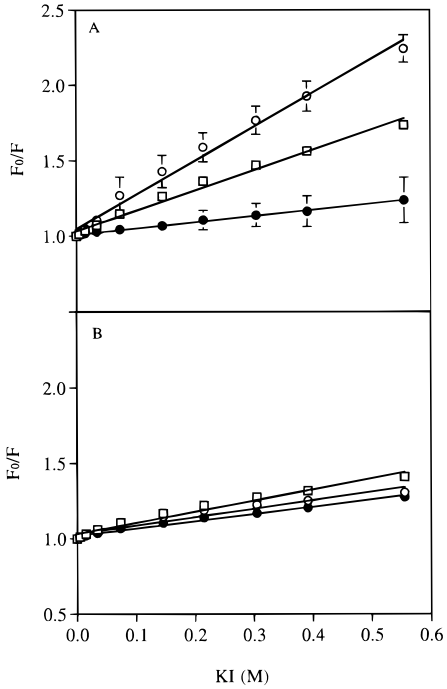

FIGURE 4: Trp fluorescence quenching in apoLp-IIIs by KI. (A) Stern−Volmer plot of KI quenching of lipid-free wild-type apoLp-III (□), apoLp-III−W@115 (●), and apoLp-III−W@130 (○). The relative quenching (F_0/F) was plotted as a function of increasing amounts of KI. Samples were excited at 295 nm and monitored between 300 and 450 nm. Values are the mean of three independent measurements ± SD. (B) Stern−Volmer plots of wild-type and mutant apoLp-III complexed with DMPC.

in a decrease of all apoLp-III K_{sv} constants to ∼0.4 M^{-1}, implying lower accessibility of the quencher.

Near-UV CD Spectra. Near-UV (250−320 nm) CD spectroscopy provides information on the environment of aromatic residues in folded proteins. In wild-type apoLp-III, the two Trp and two Phe residues give rise to the very well-defined vibronic transitions observed (*19*) (Figure 6). Extrema between 270 and 300 nm can be assigned to Trp, while the weaker Phe vibronic regions are found between 250 and 270 nm (*24*, *25*). The Phe residues are buried and located in helix 2 (Phe51) and helix 3 (Phe80). Trp extrema at 278, 286, and 292 nm observed for wild-type apoLp-III were clearly visible in apoLp-III−W@115 but were noticeably absent in apoLp-III−W@130. In the latter variant, Phe vibronic regions were resolved to a greater extent. The absence of Trp extrema at 272, 286, and 292 nm in lipid-free apoLp-III−W@130 indicates a greater flexibility in side-chain mobility of Trp130. Thus, Trp extrema in wild-type apoLp-III can be entirely assigned to Trp115, which is likely more constrained since it is buried inside the helix bundle (*4*). Upon association with DMPC, the extrema are reversed in sign, becoming entirely negative with troughs at 269, 278, 287, and 294 nm. In contrast to the lipid-free state, the lipid-bound form of apoLp-III−W@130 strongly contributes to the Trp vibronic region, indicating reduced side-chain mobility of Trp130 when complexed with lipid.

DISCUSSION

The use of Trp as an intrinsic fluorescent probe can yield considerable structural and functional information about peptides and proteins (*26*). This is particularly interesting

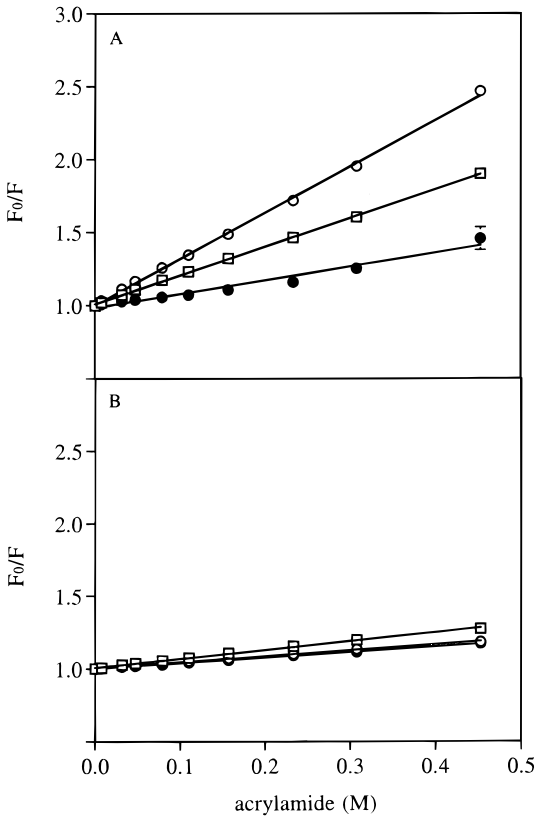

FIGURE 5: Trp fluorescence quenching in apoLp-III by acrylamide. (A) Stern−Volmer plots of lipid-free wild-type apoLp-III (□), apoLp-III−W@115 (●), and apoLp-III−W@130 (○). Values are the mean of three independent measurements ± SD. (B) Stern−Volmer plot of wild-type and mutant apoLp-IIIs complexed with DMPC.

Table 3: Trp Fluorescence Quenching of ApoLp-III in the Presence and Absence of Lipid[a]

apoLp-III	K_{sv} (M^{-1})	
	KI	acrylamide
wild type	1.35	1.96
wild type−DMPC	0.74	0.61
W@115	0.42	0.94
W@115−DMPC	0.49	0.37
W@130	2.25	3.17
W@130−DMPC	0.56	0.41

[a] Determined as described under Materials and Methods.

for exchangeable apolipoproteins since detailed structural information of lipid-binding-induced conformational changes is absent. Because of its hydrophobic nature, it is most likely that Trp residues interact directly with the lipid milieu, which generally manifests changes in fluorescence intensity, wavelength of maximum emission, and accessibility to quenchers. We exploited the fact that the two Trp residues of *L. migratoria* apoLp-III reside in unique locations in the protein, offering probes localized to a helical segment (Trp115) as well as a loop connecting helices (Trp130). Site-directed mutagenesis was performed to create mutant apoLp-IIIs with a single Trp residue at position 115 or 130. The Trp residues were converted to Phe to minimize changes in protein structure, while the contribution of Phe fluorescence to Trp fluorescence spectra is negligible. To study the proteins in the lipid bound form, apoLp-III was complexed with DMPC, resulting in formation of discoidal DMPC-apoLp-III complexes (*27*). This permits Trp fluorescence measurements without interference from other apolipoprotein components of natural lipoprotein substrates.

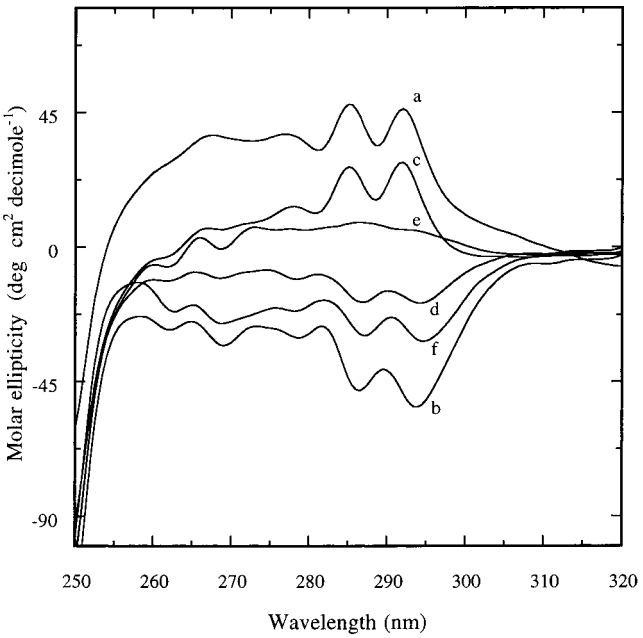

FIGURE 6: Near-UV CD spectra of lipid-free and DMPC-bound apoLp-III. Shown are wild-type apoLp-III in the absence (curve a) or presence (curve b) of DMPC, apoLp-III−W@115 in the absence (curve c) or presence (curve d) of DMPC, and apoLp-III−W@130 in the absence (curve e) or presence (curve f) of DMPC.

Structural and Functional Analysis. Minor differences in the GdnHCl-induced transition midpoint of apoLp-III−W@115 and apoLp-III−W@130 were observed (0.42 and 0.52 M, respectively), compared to wild-type apoLp-III (0.58 M). In addition, $\Delta G_D^{H_2O}$ values of the mutants were lower than that of the wild-type protein but were within the range observed for other exchangeable apolipoproteins, including *M. sexta* apoLp-III (1.29 kcal/mol; *28*) and human apoA-I (4.2 kcal/mol; *29*). These data indicate that the structural integrity of the protein has not been compromised by the mutations. This conclusion was further supported by the ability of mutant apoLp-IIIs to transform DMPC vesicles into discoidal apoLp-III-DMPC complexes at rates similar to that observed for wild-type protein. Studies of human apoA-I showed that substitution of Trp by Phe resulted in a small decrease in $\Delta G_D^{H_2O}$, while subsequent mutations resulted in lowering the stability of the protein (*30*). Those Trp residues, located in the N-terminal part of apoA-I, were suggested to play a role in stability. Furthermore, the mutations resulted in a decrease in the rate of the transition of vesicles into disclike complexes, suggesting a role for Trp in anchoring apoA-I to the DMPC surface. We found no evidence for such a function of the Trp residues in apoLp-III.

Environment of Tryptophan in ApoLp-III. The λ_{max} of Trp fluorescence of proteins varies greatly and ranges from 308 nm reported for azurin to ~350 nm of glucagon (*31*). In general, a low λ_{max} indicates a Trp buried inside the protein interior while a high λ_{max} indicates solvent exposure. For example, free L-Trp is fully solvent-exposed and displays a λ_{max} of 351 nm. A λ_{max} of 321 nm was observed for apoLp-III−W@115, while a λ_{max} of 338 nm was found for apoLp-

III−W@130. When Trp115 or Trp130 is located in fragments generated by trypsin digestion of wild-type apoLp-III, the λ_{max} is similar to that of L-Trp, indicating full exposure. The lower quantum yields observed for these peptides is most likely caused by quenching of the indole ring by peptide bonds (*31*). Quantum yields increase when either Trp is present in intact apoLp-III. The observed differences in λ_{max} indicate that Trp115 resides in a nonpolar environment while Trp130 is partially solvent-exposed. Thus, protein folding relocates these Trp residues to different environments, resulting in manifestation of distinct fluorescence properties. According to high-resolution structural data (*4*), Trp115 is buried, directing its indole ring toward the hydrophobic interior of the helical bundle, which explains the highly blue-shifted λ_{max} (Figure 1). On the other hand, Trp130 resides in the short loop connecting helices 4 and 5 that is postulated to serve as a hinge during conformational opening of the helix bundle when the protein binds to lipid (*19*). Complexation of apoLp-III with DMPC resulted in a blue shift for Trp130 (338 to 331 nm) and a red shift for Trp115 (321 to 327 nm). This implies relocation of both fluorophores to a new, similar environment when bound to DMPC.

Quenching Studies. ApoLp-III−W@130 has a considerably higher KI quenching constant than apoLp-III−W@115 (2.25 M^{-1} and 0.42 M^{-1}, respectively), implying that Trp130 is more exposed. For comparison, free L-Trp has a K_{sv} of 11.6 M^{-1} (*23*). According to DSSP analysis (*32*) of the X-ray coordinates (Brookhaven Protein Data Bank, code 1AEP), the Trp130 side chain is only 13% solvent-accessible (0% for Trp115). However, the relatively high thermal factor of Trp130 indicates flexibility of this tryptophan that might explain its higher accessibility to quenching and its relatively greater exposure to the aqueous environment. The difference in K_{sv} values in the lipid-free state becomes much smaller when the protein binds to DMPC ($\sim$ 0.5 M^{-1}). In the case of acrylamide, the K_{sv} for apoLp-III−W@115 upon lipid binding decreased from 0.94 to 0.37 M^{-1}, while K_{sv} for apoLp-III−W@130 was reduced from 3.17 to 0.41 M^{-1}. Both Trp115 and Trp130 are less accessible when the protein adopts the lipid-bound conformation, indicating both Trp residues are in close proximity to the new lipid environment. In this respect, it is noteworthy that Trp residues of many membrane proteins have a preferred orientation near the lipid−water interface (*33*).

Comparison with Other Exchangeable Apolipoproteins. Several studies have been reported that used tryptophan fluorescence as a tool to investigate changes in the structure of exchangeable apolipoproteins upon binding to a lipid surface. As shown in Table 4, *Bombyx mori* apoLp-III is a single-Trp apolipoprotein that, upon lipid binding, shows a strong blue shift (*34*). The single Trp of human apoC-I is fully exposed to buffer (λ_{max} 353 nm) but the DMPC-bound form shows a large blue shift to 337 nm (*35*). This was also reflected by a substantial decrease in KI quenching. Human proapoA-I contains five Trp residues, and single-Trp mutants showed λ_{max} values between 332 and 338 nm. The proapoA-I mutants in reconstituted HDL underwent a blue shift in the order of 1−6 nm in addition to lower accessibility to KI quenching (*36*). Binding of chicken apoA-I (bearing two Trp residues) to DMPC did not result in a change in λ_{max}, which remained at 331 nm (*37*). For human apoE, a 5 nm blue shift occurred upon binding to DMPC. This could be attributed to the C-terminal domain of the protein, which undergoes a blue shift in λ_{max} from 341 to 332 nm (*38*, *39*), while the λ_{max} of the N-terminal domain of apoE shifts from 342 to 341 nm when bound to DMPC. This indicates that the four Trp residues of the N-terminal domain of apoE remained partially exposed to solvent. Another explanation is that the sum of the fluorescence of those Trp residues in N-terminal apoE mask individual changes as seen in *L. migratoria* apoLp-III. This underlines the importance of studying Trp fluorescence of single-Trp proteins to probe changes in their environment as a result of conformational changes. Such proteins can be generated by site-directed mutagenesis and produced by various expression systems. From the data summarized in Table 4 it is observed that λ_{max} values of Trp residues in exchangeable apolipoproteins vary between a wide range of 321 and 353 nm, implying that these amino acids reside anywhere in the protein, either completely buried in the protein interior or with varying degrees of exposure to the aqueous environment. In most cases, lipid binding of apolipoproteins induces a shift in λ_{max} toward a narrow range of 330−338 nm, which indicates Trp residues localize to a hydrophobic environment such as the lipid milieu. The change in λ_{max} is generally accompanied by a decrease in quencher accessibility.

Table 4: Wavelength of Trp Fluorescence Emission Maximum (λ_{max}) of Exchangeable Apolipoproteins in the Lipid-Free and Lipid-Bound States

exchangeable apolipoprotein[a]	number of Trp residues	λ_{max} (nm)		ref
		lipid-free	lipid-bound	
apoLp-III (*L.m.*)	2	332	329	
apoLp-III−W@115 (*L.m.*)	1	321	327	
apoLp-III−W@130 (*L.m.*)	1	338	331	
apoLp-III (*B.m.*)	1	327	311	*34*
apoC−I (h)	1	353	337	*35*
proapoA-I (h)	5	336	335	*36*
proapoA-I mutants (h)	1	332−338	330−336	*36*
apoAI (chicken)	2	331	331	*37*
apoE (h)[b]	7	343	338	*38*, *39*
apoE, C-terminal domain	2	341	332	*38*, *39*
apoE, N-terminal domain	4	342	341	*38*, *39*

[a] Apolipoproteins listed are from *Locusta migratoria* (*L.m.*), *Bombyx mori* (*B.m.*), human (h), and chicken (*Gallus domesticus*). [b] The loop region connecting N- and C-terminal domains of apoE contains one Trp residue.

Aromatic Circular Dichroism. Near-UV CD spectra of apoLp-III provided information about the environment of Trp and Phe residues. Extrema were observed at 268, 278, 286, and 292 nm for wild type and apoLp-III−W@115. For apoLp-III−W@130 the spectrum was less well-defined, lacking strong Trp vibronic bands. However, the Phe regions were well defined with extrema at 260 and 266 nm. The lack of Trp extrema and the presence of a third Phe residue inside the helix bundle may contribute to the Phe vibronic regions. The lack of the Trp vibronic bands in apoLp-III−W@130 indicates that Trp130 is in a less constrained environment, in accordance with its location in the loop region (Figure 1). Upon lipid binding, the vibronic bands are reversed in sign becoming negative with extrema at 262, 269, 278, 287, and 294 nm. The Phe vibronic regions are resolved better in the lipid-bound form compared to lipid-free apoLp-III. Importantly, strong Trp vibronic bands at 287

and 294 nm are visible for lipid-associated apoLp-III−W@130. Thus, interaction with lipid localizes Trp130 to a more rigid environment. Restriction of its side-chain mobility is responsible for the observed strong extrema in this case (*24*). Both apoLp-III−W@115 and apoLp-III−W@130 show a similar aromatic CD spectrum in the presence of lipid, indicating that both residues localize to similar environments. The shift to longer wavelength indicates that Trp is in a more nonpolar environment (*25*).

Concluding Remarks. Changes in λ_{max}, quencher accessibility for KI and acrylamide, and aromatic CD spectral properties indicate that both Trp115 and Trp130 of *L. migratoria* apoLp-III relocate to a lipid environment upon association with DMPC. Although no high-resolution data are available for the conformation of apoLp-III bound to DMPC, experimental evidence suggest that the protein adopts an open conformation, circumscribing the periphery of the discs, arranging the α-helices perpendicular to the fatty acyl chains of the phospholipids (*11*, *18*, *19*). It is most likely that the side chains of hydrophobic amino acid residues, including Trp, interact directly with the lipid surface. This explains why both Trp residues display similar fluorescence properties when complexed with lipid. The hydrophobic face of helix 4 most likely interacts directly with the exposed lipid surface. Importantly, this study also shows that the loop Trp interacts with the hydrophobic surface similar to that of the helix-associated Trp. It is conceivable that lipid binding induces helical character in the loop between helices 4 and 5, resulting in an extended α-helix, analogous to the belt model proposed for apoA-I (*6*). Indeed, this may be one of the driving forces behind the conformational change when the protein adopts the "open" state upon lipid binding.

ACKNOWLEDGMENT

We thank Kim Oikawa and Robert Luty for assistance in CD spectroscopy and Paul Semchuk for mass spectrometry.

REFERENCES

1. Van der Horst, D. J. (1990) *Biochim. Biophys. Acta 1047*, 195−211.
2. Blacklock, B. J., and Ryan, R. O. (1994) *Insect Biochem. Mol. Biol. 24*, 855−873.
3. Soulages, J. L., and Wells, M. A. (1994) *Adv. Protein Chem. 45*, 371−415.
4. Breiter, D. R., Kanost, M. R., Benning, M. M., Wesenberg, G., Law, J. H., Wells, M. A., Rayment, I., and Holden, H. M. (1991) *Biochemistry 30*, 603−608.
5. Wilson, C., Wardell, M. R., Weisgraber, K. H., Mahley, R. W., and Agard, D. A. (1991) *Science 252*, 1817−1822.
6. Borhani, D. W., Rogerts, D. P., Engler, J. A., and Brouillette, C. G. (1997) *Proc. Natl. Acad. Sci. U.S.A. 94*, 12291−12296.
7. Wang, J., Gagné, S. M., Sykes, B. D., and Ryan, R. O. (1997) *J. Biol. Chem. 272*, 17912−17920.
8. Jonas, A. (1992) in *Structure and Function of Apolipoproteins* (Rosseneu, M., Ed) pp 217−250, CRC Press Inc., Boca Raton, FL.
9. Roberts, L. M., Ray, M. J., Shih, T., Hayden, E., Reader, M. M., and Brouillette, C. G. (1997) *Biochemistry 36*, 7615−7624.
10. Raussens, V., Fisher, C. A., Goormaghtigh, E., Ryan, R. O., and Ruysschaert, J.-M. (1998) *J. Biol. Chem. 273*, 25825−25830.
11. Raussens, V., Narayanaswami, V., Goormaghtigh, E., Ryan, R. O., and Ruysschaert, J.-M. (1995) *J. Biol. Chem. 270*, 12542−12547.
12. Ryan, R. O., Schieve, D., Wientzek, M., Narayanaswami, V., Oikawa, K., Kay, C. M., and Agellon, L. (1995) *J. Lipid Res. 36*, 1066−1072.
13. Weers, P. M. M., Wang, J., Van der Horst, D. J., Kay, C. M., Sykes, B. D., and Ryan, R. O. (1998) *Biochim. Biophys. Acta 1393*, 99−107.
14. Narayanaswami, V., and Ryan, R. O. (2000) *Biochim. Biophys. Acta 1483*, 15−36.
15. Narayanaswami, V., Wang, J., Kay, C. M., Scraba, D. G., and Ryan, R. O. (1996) *J. Biol. Chem. 271*, 26855−26862.
16. Narayanaswami, Wang, J., Schieve, D, Kay, C. M., and Ryan, R. O. (1999) *Proc. Natl. Acad. Sci. U.S.A. 94*, 12291−12296.
17. Weers, P. M. M., Narayanaswami, V., Kay, C. M., and Ryan, R. O. (1999) *J. Biol. Chem. 274*, 21804−21810.
18. Wientzek, M., Kay, C. M., Oikawa, K., and Ryan, R. O. (1994) *J. Biol. Chem. 269*, 4605−4612.
19. Weers, P. M. M., Kay, C. M., Oikawa, K., Wientzek, M., Van der Horst, D. J., and Ryan, R. O. (1994) *Biochemistry 33*, 3617−3624.
20. Sanger, F., Nicklen, S., and Coulson, A. R. (1977) *Proc. Natl. Acad. Sci. U.S.A. 74*, 5463−5467.
21. Surewicz, W., Epand, R. M., Pownall, H. J., and Hiu, S.-K. (1986) *J. Biol. Chem. 261*, 16191−16197.
22. Provencher, S. W., and Glöckner, J. (1981) *Biochemistry 20*, 33−37.
23. Lehrer, S. S. (1971) *Biochemistry 10*, 3254−3263.
24. Strickland, E. H. (1974) *CRC Crit. Rev. Biochem. 2*, 113−175.
25. Lux, S. E., Hirz, R., Shrager, R. I., and Gotto, A. M. (1972) *J. Biol. Chem. 247*, 2598−2606.
26. Eftink, M. R. (1991) *Methods Biochem. Anal. 35*, 127−205.
27. Weers, P. M. M., Van der Horst, D. J., and Ryan, R. O. (2000) *J. Lipid Res. 41*, 416−423.
28. Ryan, R. O., Oikawa, K., and Kay, C. M. (1993) *J. Biol. Chem. 268*, 1525−1530.
29. Reijngoud, D. J., and Phillips, M. C. (1982) *Biochemistry 21*, 2969−2976.
30. Davidson, W. S., McGuire, K. A., and Jonas, A. (1998) in *Atherosclerosis XI* (Jacotot, B., Mathé, D., and Fruchart, J.-C., Eds.) pp 1135−1142, Elsevier Science Pte Ltd., Singapore.
31. Schiller, P. W. (1985) in *The Peptides*, Vol. 7, pp 115−164, Academic Press Inc., San Diego, CA.
32. Kabsch, W., and Sander, S. (1983) *Biopolymers 22*, 2577−2637.
33. Mukherjee, S., and Chattopadhyay, A. (1994) *Biochemistry 33*, 5089−5097.
34. Narayanaswami, V., Yamauchi, Y., Weers, P. M. M., Maekawa, H., Sato, R., Tsuchida, K., Oikawa, K., Kay, C. M., and Ryan, R. O. (2000) *Eur. J. Biochem, 267*, 728−736.
35. Jonas, A., Privat, J.-P., Wahl, P., and Osborne, J. C., Jr. (1982) *Biochemistry 21*, 6205−6211.
36. Davidson, W. S., Arnvig-McGuire, K., Kenney, A., Kosman, J., Hazlett, T. L., and Jonas, A. (1999) *Biochemistry 38*, 14387−14395.
37. Kiss, R. S., Kay, C. M., and Ryan, R. O. (1999) *Biochemistry 38*, 4327−4334.
38. Aggerbeck, L. P., Wetterau, J. R., Weisgraber, K. H., Wu, C.-S. C., and Lindgren, F. T. (1988) *J. Biol. Chem. 263*, 6249−6258.
39. de Pauw, M., Vanloo, B., Weisgraber, K. H., and Rosseneu, M. (1995) *Biochemistry 34*, 10953−10960.

BI992891X